

Exploiting Conformational Dynamics To Facilitate Formation and Trapping of Electron-Transfer Photoproducts in Metal Complexes

Heather A. Meylemans, Joshua T. Hewitt, Mirvat Abdelhaq, Paul J. Vallett, and Niels H. Damrauer*

Department of Chemistry and Biochemistry, University of Colorado at Boulder, Boulder, Colorado 80309

Received June 24, 2010; E-mail: niels.damrauer@colorado.edu

Abstract: Three new photoinduced electron donor–acceptor (D–A) systems are reported which juxtapose a Ru(II) excited-state donor with a bipyridinium acceptor via a conformationally active asymmetric aryl-substituted bipyridine ligand participating in the bridge between D and A. Across the series of complexes **1–3**, steric bulk is sequentially added to tune the inter-ring dihedral angle θ between the bipyridine and the aryl substituent. Driving forces for photoinduced electron transfer (ΔG_{ET}) and back electron transfer (ΔG_{BET}) are reported based on electrochemical measurements of **1–3** as well as Franck–Condon analysis of emission spectra collected for three new donor model complexes **1'–3'**. These preserve the substitution patterns on the aryl substituent in their respective D–A complexes but remove the bipyridinium acceptor. Both ΔG_{ET} and ΔG_{BET} are invariant to within 0.02 eV across the series. Upon visible photoexcitation of each of the D–A systems with ~ 100 fs laser pulses at 500 ± 10 nm, an electron-transfer (ET) photoproduct is observed to form with a time constant of $\tau_{\text{ET}} = 29$ ps (**1**), 37 ps (**2**), and 57 ps (**3**). That ET remains relatively rapid throughout this series, even as steric bulk significantly increases the inter-ring dihedral angle θ , is attributed to the effects of ligand-based torsional dynamics driven by intraligand electron delocalization in the $D^*–A$ excited state manifold prior to ET. The lifetimes of the charge-separated states (τ_{BET}) are also reported with $\tau_{\text{BET}} = 98$ ps (**1**), 217 ps (**2**), and 789 ps (**3**), representing a more than 8-fold increase across the series. This is attributed to reverse conformational dynamics in $D^+–A^-$ driven by steric repulsions, which serves to minimize electronic coupling to the ground state. Steric control of ligand geometry and the range over which θ changes during conformational dynamics provides a new strategy to facilitate the formation and storage of charge-separated excited states.

Electron transfer (ET) research exploiting structural manipulations of donor–acceptor (D–A) systems has expanded our fundamental understanding of reactivity between electronic states and has guided strategies for solar energy conversion.¹ We have been interested in developing D–A design principles wherein excited-state conformational dynamics on low-frequency nuclear modes that are nominally orthogonal to high-frequency ET reaction coordinates are exploited to both facilitate charge separation (ET) and hinder energy wasting recombination reactions (back electron transfer, BET).^{2,3} Ideal systems would avoid relying on driving force and ET distance to create and store charge-separated states, thus circumventing a key source of inefficiency common to both synthetic and natural solar energy conversion strategies. Our approach exploits the general concept that thermally accessible nuclear motions can impact intercomponent electronic couplings important for determining rates of ET, exchange-mediated energy

transfer, and conduction in molecular systems^{4–12} (see ref 3 for a more extensive bibliography).

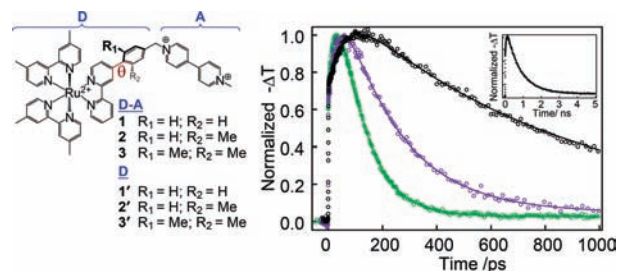


Figure 1. (Left) D–A and respective D complexes with varying steric bulk on the conformationally active aryl substituent (θ indicated in red). (Right) Representative transient absorption kinetics collected for **1** (green), **2** (purple), and **3** (black) in acetonitrile at 294 K at $\lambda_{\text{probe}} = 607$ nm following ~ 100 fs pulsed excitation at 500 nm. Solid lines are fits of the data to a biexponential model (rise and decay). (Right inset) Transient and fit for **3** expanded to 5 ns.

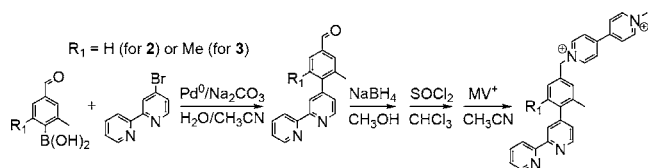
Of recent interest in our group are systems (see Figure 1 for species explored herein) that juxtapose a Ru(II) excited-state donor with a bipyridinium acceptor via a conformationally active asymmetric aryl-substituted bipyridine ligand serving as the bridge. Diquaternary ammonium acceptors are commonly used for both bimolecular and unimolecular ET studies with d^6 transition metal donor complexes (e.g., refs 1, 13, and 14). In our systems metal-to-ligand charge-transfer (MLCT) states populating the π^* system of the asymmetric ligand are expected to initiate ligand-based molecular geometry changes along torsional nuclear coordinates, i.e., planarization of θ (we consider the absolute value of this quantity θ between 0° and 90°) driven by excited-state intraligand electron delocalization.^{2,15} Such motions can facilitate ET if they (a) lower the reorganization energy in the $D^*–A \rightarrow D^+–A^-$ reaction, as we have previously argued to be important,² and/or (b) change the electronic coupling between these states, both by varying the distance of ET and by tuning superexchange through orbital overlap changes.³ Opportunities to hinder BET arise if reverse motions, driven by steric effects, decrease electronic coupling between $D^+–A^-$ and D–A states.

Recent computational work from our group explored structure and excited-state conformational activity of these systems.³ In DFT models of **1**, **2**, and **3**, $\theta = 35^\circ$, 50° , and 86° , respectively, for ground-state and, by inference, the Franck–Condon state geometries. The vibrationally relaxed ³MLCT states were also modeled, leading to the finding that each species has a more planarized aryl substituent relative to the bipyridine in the excited state prior to ET by 13° (**1**), 15° (**2**), and 31° (**3**). While we expect k_{ET} to decrease across the series as electronic communication between D and A through the π^* system is diminished (as θ increases), the planarizing torsional motion can limit the effects and ideally permit facile ET in each of the systems.

A second important conclusion from computational models is that complete or nearly complete *reverse* switching of θ is expected following the formation of the ET photoproduct D^+A^- . An optimized geometry where $\theta = 33^\circ$ was previously reported for the lowest energy triplet state (namely, D^+A^-) of **1**.³ Similar calculations (B3LYP functional with PCM acetonitrile continuum; basis set identical to ref 3)¹⁶ were carried out here for **2** and **3** with comparable results: for **2**, $\theta = 47^\circ$ whereas for **3**, $\theta = 88^\circ$. Thus θ is expected to be approximately the same for both the ground state and the ET product for **1–3**. A simplistic model for tuning electronic coupling between reactant (D^+A^-) and product ($D-A$) states for the BET reaction suggests important consequences of these reverse switching motions. If coupling is proportional to $\cos(\theta)$, as is expected from superexchange treatments of biaryl ET bridges,^{3,7,10,17} then k_{BET} would be strongly affected when reverse switching motions reach larger values of θ such as that predicted in **3**.

To measure the effects of geometry and torsion-conformational dynamics on k_{ET} and k_{BET} , we have synthesized compounds **1–3**. The asymmetric electroactive ligand needed for **1** has been reported by us.² Those needed for **2** and **3** were synthesized according to Scheme 1. Donor complexes **1'–3'** were also synthesized which preserve the methyl substitution pattern on the aryl group but remove the bipyridinium acceptor. These are used to estimate the stored ³MLCT excited-state energy prior to ET. As shown in Figures S1–S3 (Supporting Information), there is excellent agreement between the absorption spectra of each donor model and the respective D–A complex, thus justifying their use. ¹H NMR chemical shifts and accurate mass spectrum analyses for **1–3** and **1'–3'** as PF₆[−] salts are reported in the Supporting Information.

Scheme 1. Synthetic Strategy for Electroactive Ligands in **2** and **3**



The driving forces for ET and BET in **1–3** have been determined through electrochemical measurements (see Table S1, Supporting Information) and through emission spectroscopy of the donor models **1'–3'** (see Figures S1–S3). Franck–Condon analysis¹⁸ yields ΔG_{MLCT} as a measure of the stored energy in the long-lived ³MLCT of the donor models and therefore the stored excited-state energy in **1–3** prior to ET (Table S1). The first oxidation and reduction potentials measured for **1–3** allow for the determination of the free energy of formation of the ion-pair state D^+A^- (ΔG_{IP}).¹⁹ The quantities ΔG_{IP} and ΔG_{MLCT} are used to determine $\Delta G_{\text{ET}} (= -\Delta G_{\text{MLCT}} + \Delta G_{\text{IP}})$ and $\Delta G_{\text{BET}} (= -\Delta G_{\text{IP}})$ listed in Table 1. As can be seen, there is little variation in either ΔG_{ET} or ΔG_{BET} for **1–3**. This is an ideal situation in efforts to unravel specific effects of the bridging-ligand geometry and torsional dynamics on k_{ET} and k_{BET} in a structural series of D–A complexes.

Transient absorption spectroscopy with ~ 100 fs time resolution has been utilized to measure ET rate constants for **1–3** in acetonitrile at 294 K. Here we focus on single-wavelength kinetics (Figure 1) at $\lambda_{\text{probe}} = 607$ nm following short-pulse excitation into the MLCT band at $\lambda_{\text{pump}} = 500$ nm. The probe wavelength was chosen in order to interrogate the well-known visible absorption of the radical formed when MV^{2+} is reduced by one electron.² Reductive spectroelectrochemistry on **1–3** confirms this expectation (see Figures S4–S6, Supporting Information). Compound **1** shows

Table 1. Measured ET Properties in Acetonitrile

	1	2	3
$\Delta G_{\text{ET}} / \text{eV}$	−0.58	−0.58	−0.59
$\Delta G_{\text{BET}} / \text{eV}$	−1.53	−1.55	−1.55
$k_{\text{ET}}^a / 10^{10} \text{ s}^{-1}$	3.4 ± 0.2	2.7 ± 0.1	1.75 ± 0.1
$\tau_{\text{ET}} / \text{ps}$	29 ± 2	37 ± 2	57 ± 3
$k_{\text{BET}}^a / 10^{10} \text{ s}^{-1}$	1.02 ± 0.03	0.46 ± 0.01	0.127 ± 0.002
$\tau_{\text{BET}} / \text{ps}$	98 ± 3	217 ± 4	789 ± 9

^a Rate constants from data collected at 294 K. Error bars represent 2σ determined from fitting three separate measurements of kinetics collected at $\lambda_{\text{probe}} = 607$ nm.

a rise in the transient absorption intensity with a time constant of 29 ps (τ_{rise}), followed by a decay of 98 ps (τ_{decay}). These kinetics are understood in the context of observations and analysis by our group on related bis-heteroleptic D–A species where the ancillary ligand (L) is modified to tune ΔG_{ET} and ΔG_{BET} .² For example, changing L from 2,2'-bipyridine (bpy) to 4,4',5,5'-tetramethyl-2,2'-bipyridine (tmb) is accompanied by a modification in ΔG_{BET} from -1.7 to -1.5 eV and a decrease in τ_{decay} ($\lambda_{\text{probe}} = 607$ nm kinetics) from 160 to 73 ps. This is the expected result for Marcus inverted region kinetics which allows us to assign τ_{decay} to τ_{BET} and, by inference, τ_{rise} to τ_{ET} . Kinetics collected for **1–3** at 400 nm (also containing MV^+ absorption) and 460 nm (MLCT bleach) behave as expected.

The systematic introduction of steric bulk at the aryl substituent of the asymmetric ligand has the effect of increasing τ_{ET} by about a factor of 2 across the series **1–3** (from 29 ps (**1**) to 57 ps (**3**)). The structural modifications appear responsible, which in and of itself is an important finding. It is emphasized, however, that the increase in τ_{ET} across the series is modest in light of the significant ground-state structural differences of the bridging ligand with respect to θ (vide supra). Here we believe that intraligand electron delocalization^{2,15} in D^*A^- prior to ET, the effect which drives the predicted decrease in θ in the ³MLCT states, plays a critical role, facilitating ET even in the most sterically encumbered system **3**. This finding is consistent with calculations of the ³MLCT states of **1'–3'** showing spin population on the aryl substituent in each of these systems.³

Importantly, whereas τ_{ET} for the sterically encumbered **3** increases by less than a factor of 2 relative to **1**, τ_{BET} increases by more than a factor of 8 (from 98 ps (**1**) to 789 ps (**3**)). This leads to the dramatic lengthening of the transient absorption decay for **3** versus **1** shown in Figure 1. The ratio between the lifetime of charge separation (τ_{BET}) and the time it takes to achieve it (τ_{ET}) may be considered as a figure of merit. Here the structural and dynamical modifications put in place across the series allow for substantial tuning of $\tau_{\text{BET}}/\tau_{\text{ET}}$ from 3.4 in **1** to 5.9 in **2** to 14 in **3**. The very favorable properties of **3** in terms of this ratio are interpreted to be a consequence of the range over which excited-state torsional motions occur. The initial planarization of the dihedral angle by 31° , driven by intraligand electron delocalization, is sufficient to achieve electronic coupling that permits relatively efficient forward ET. By contrast, the energy-wasting BET is inefficient. The reverse switching driven by steric repulsions accesses a dihedral angle ($\theta = 88^\circ$) where the reduced acceptor (MV^+) is significantly decoupled from the Ru(III) center through the π^* system of the bridging ligand. Notably, with electronic coupling proportional to $\cos(\theta)$, the range over which θ changes in **3** permits a significantly stronger contrast between τ_{BET} and τ_{ET} than in either **1** or **2** (see also discussion in ref 3). The electronic coupling is of course nonzero, as evidenced by the finite lifetime $\tau_{\text{BET}} = 789$ ps. Through-solvent coupling may play a role.²⁰ Further, at 294 K a range of dihedral angles will be thermally accessible, leading to larger electronic coupling. Finally,

ET pathways where orbital symmetry dictates that $\theta = 90^\circ$ is not the electronic coupling minimum may participate, as has been observed in bis-porphyrin systems.⁶ Additional computational efforts are needed to explore these points in greater detail.

These results demonstrate that synthetic design principles, guided by measurement and prediction of excited-state dynamics on low-frequency vibrational coordinates, can be used to increase the lifetime of ET photoproducts without greatly reducing their rate of formation. Researchers interested in charge separation at interfaces while avoiding recombination reactions — a topic critical to the development of solar energy conversion strategies — may want to consider use of what may appear to be an unlikely choice: namely, π -systems for which conjugation appears restricted due to the influence of steric repulsions on inter-ring dihedral angles. In our laboratory, temperature-dependent experiments are underway to establish values of electronic coupling for the ET and BET reactions in this series.

Acknowledgment. This work was supported by the National Science Foundation under CHE-0847216. Computational resources were due to the NSF through their NCSA TeraGrid.

Supporting Information Available: Synthetic, experimental, and data fitting procedures; ¹H NMR shifts, accurate mass spectrum analyses, and absorption and emission spectra for new compounds; spectroelectrochemical data, XYZ coordinates, and computational

details; complete ref 16. This material is available free of charge via the Internet at <http://pubs.acs.org>.

References

- (1) *Electron Transfer in Chemistry*; Balzani, V., Ed.; Wiley-VCH: Weinheim, 2001.
- (2) Meylemans, H. A.; Lei, C. F.; Damrauer, N. H. *Inorg. Chem.* **2008**, *47*, 4060.
- (3) Meylemans, H. A.; Damrauer, N. H. *Inorg. Chem.* **2009**, *48*, 11161.
- (4) Ratner, M. A.; Madhukar, A. *Chem. Phys.* **1978**, *30*, 201.
- (5) Hoffman, B. M.; Ratner, M. A. *J. Am. Chem. Soc.* **1987**, *109*, 6237.
- (6) Helms, A.; Heiler, D.; McLendon, G. *J. Am. Chem. Soc.* **1991**, *113*, 4325.
- (7) Davis, W. B.; Ratner, M. A.; Wasielewski, M. R. *J. Am. Chem. Soc.* **2001**, *123*, 7877.
- (8) Weiss, E. A.; Tauber, M. J.; Kelley, R. F.; Ahrens, M. J.; Ratner, M. A.; Wasielewski, M. R. *J. Am. Chem. Soc.* **2005**, *127*, 11842.
- (9) Laine, P. P.; Bedioui, F.; Loiseau, F.; Chiorboli, C.; Campagna, S. *J. Am. Chem. Soc.* **2006**, *128*, 7510.
- (10) Benniston, A. C.; Harriman, A. *Chem. Soc. Rev.* **2006**, *35*, 169.
- (11) Eng, M. P.; Martensson, J.; Albinsson, B. *Chem. Eur. J.* **2008**, *14*, 2819.
- (12) Huynh, M. H. V.; Meyer, T. J. *Chem. Rev.* **2007**, *107*, 5004.
- (13) Yonemoto, E. H.; Saupe, G. B.; Schmehl, R. H.; Hubig, S. M.; Riley, R. L.; Iverson, B. L.; Mallouk, T. E. *J. Am. Chem. Soc.* **1994**, *116*, 4786.
- (14) Weber, J. M.; Rawls, M. T.; MacKenzie, V. J.; Limoges, B. R.; Elliott, C. M. *J. Am. Chem. Soc.* **2007**, *129*, 313.
- (15) Damrauer, N. H.; Boussie, T. R.; Devenney, M.; McCusker, J. K. *J. Am. Chem. Soc.* **1997**, *119*, 8253.
- (16) Frisch, M. J.; et al. *Gaussian 09*, Revision A.1; Gaussian, Inc.: Wallingford, CT, 2009.
- (17) McConnell, H. J. *Chem. Phys.* **1961**, *35*, 508.
- (18) Kober, E. M.; Caspar, J. V.; Lumpkin, R. S.; Meyer, T. J. *J. Phys. Chem.* **1986**, *90*, 3722.
- (19) Weller, A. *Z. Phys. Chem.* **1982**, *133*, 93.
- (20) Kumar, K.; Lin, Z.; Waldeck, D. H.; Zimmt, M. B. *J. Am. Chem. Soc.* **1996**, *118*, 243.

JA105559